Supplemental Document

Optics EXPRESS

Uncertainty assessment of unattended above-water radiometric data collection from research vessels with the Dynamic Above-water Radiance (L) and Irradiance (E) Collector (DALEC): supplement

David Antoine,[1,2,*] Matthew Slivkoff,[3] Wojciech Klonowski,[3] Charles Kovach,[4] and Michael Ondrusek[5]

[1]*Remote Sensing and Satellite Research Group, School of Earth and Planetary Sciences, Curtin University, Perth, WA 6845, Australia*
[2]*Sorbonne Université, CNRS, Laboratoire d'Océanographie de Villefranche, LOV, F-06230 Villefranche-sur-Mer, France*
[3]*In-situ Marine Optics Pty Ltd., Bibra Lake, WA 6163, Australia*
[4]*Global Science & Technology, Inc., Greenbelt, Maryland 20770, contractor to NOAA / NESDIS / STAR, College Park, MD 20740, USA*
[5]*NOAA / NESDIS / STAR, College Park, MD 20740, USA*
[*]*david.antoine@curtin.edu.au*

Supplement DOI: https://doi.org/10.6084/m9.figshare.13359569

Parent Article DOI: https://doi.org/10.1364/OE.412022

Uncertainty assessment of unattended above-water radiometric data collection from research vessels with the Dynamic Above-Water Radiance (L) and Irradiance (E) Collector (DALEC): supplemental document

S1. DALEC radiometric characterization and calibration

Each DALEC optical channel utilizes a collimating lens (350 nm – 2000 nm) and a 350 nm Optical Density 4 (OD4) long-pass filter in front of the spectrometer's optic fiber input. Using this configuration, ultraviolet light is adequately attenuated in the first few detector pixels and these pixels are then used to correct for the dark offset response of each spectrum.

The E_s channel incorporates a Polytetrafluoroethylene (PTFE) diffuser and achieves a typical cosine response error < 3% to 60° and < 10% to 87.5° (Fig. S1). Fused Silica windows are used for both L_u and L_s channels and the collimating optics provide a FOV of ~ 5° for each.

Temperature sensors are located on each of the Zeiss^{TM} Monolithic Miniature Spectrometers (MMS1) arrays to assist in correcting for temperature drift of the spectrometers. The pitch and roll data are utilized to quality control spectra where excessive ship motion may interfere with the measurement geometry.

Each spectrometer is calibrated separately using a National Institute of Standards and Technology (NIST)-traceable 1000W FEL lamp and stable power supply. The E_s channel is radiometrically calibrated with a direct view of the FEL lamp filament, and the L_t and L_s channels are calibrated whilst viewing a calibrated 99% reflectance Spectralon^{TM} plaque at 45 degree incidence [1]. A full set of calibrations are performed over a wide range of detector temperatures ranging from ~16°C to ~40°C and at different integration times (1, 2, 4, 8, 16, 32, 64, 128, 256, 512 ms). During calibration, the DALEC continually iterates through the set of integration times while the DALEC detectors are warming up. From this data, each spectrometers integration-time non-linearity, responsivity, temperature effects and radiometric calibration coefficients are derived.

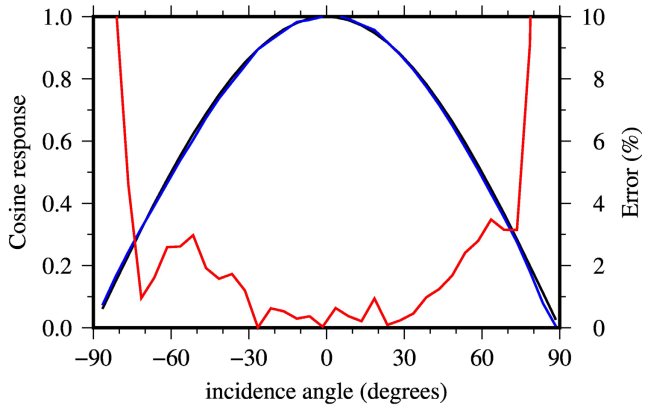

Fig. S1. Experimental DALEC cosine response (blue curve) compared to a theoretical perfect cosine response (black). The percent difference between both is displayed as the red curve (values on the right axis).

Non-linearity with respect to integration time for Zeiss MMS1 spectrometers arise from the additional photoelectron signal generated during the readout phase of the pixel array during the integration [2]. The conversion of a raw spectrum, DN_i to a dark corrected count rate, CR_i which accounts for the readout time, $\Delta t_{readout}$ (Fig. S2a), is calculated as,

$$CR_i = \frac{DCcorr_i}{Inttime + \Delta t_{readout}}, \quad (1)$$

where, $Inttime$ is the integration time in milliseconds and $DCcorr_i$ is the dark count corrected signal. The count rate (normalized to 1 @ 30,000 counts) versus dark corrected counts (Fig. S2b) shows the effect of integration time non-linearity. From this, the linearly corrected spectrum, $LinCorr_i$, is calculated as,

$$LinCorr_i = d_o DCcorr_i + d_i, \quad (2)$$

where, the coefficients d_0, d_i and Δt are derived separately for each spectrometer.

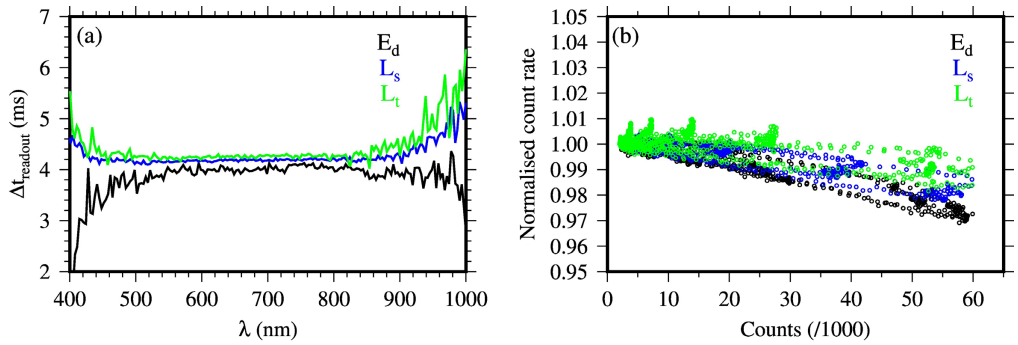

Fig. S2. (a) The $\Delta t_{readout}$ vs. wavelength for the three DALEC spectrometers, as indicated. Only the average Δt is used in the count rate calculation. (b) Count rate normalized to 1 at 10000 counts, vs. counts.

The illuminated signal response of Zeiss MMS1 spectrometers is known to change with temperature [3]. This is largely explained by the temperature response of silicon photodiodes (wavelength dependent) and, to a lesser extent, the optical components and spectrometer electronics. The derived temperature coefficients, $TEMPCO$ (normalized to 1 at 24 degrees) for each spectrometer show a small effect at blue wavelengths and increasing toward NIR wavelengths. (Fig. S3). The temperature corrected spectrum, T*corr* for pixel *i* is calculated as,

$$Tcorr_i = LinCorr_i \ [TEMPCO(T - 24) + 1] \quad (3)$$

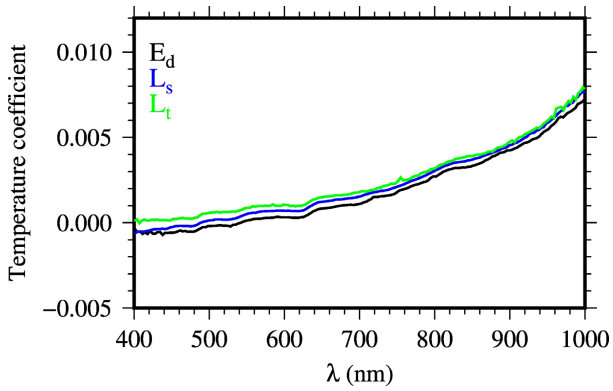

Fig. S3. Temperature coefficient of the three spectrometers as a function of wavelength.

Once the temperature effects are corrected, the radiometric responsivity calibration coefficients are used to convert the spectrometer data into engineering units, i.e.,

$$\begin{aligned} Es_i &= Fe_i \times Tcorr_i \text{ [W m}^{-2}\text{ nm}^{-1}\text{]}, \\ Lu_i &= Flu_i \times Tcorr_i \text{ [W m}^{-2}\text{ sr}^{-1}\text{ nm}^{-1}\text{]}, \\ Ls_i &= Fls_i \times Tcorr_i \text{ [W m}^{-2}\text{ sr}^{-1}\text{ nm}^{-1}\text{]}, \end{aligned} \quad (4)$$

where, F_e, Fl_u and Fl_s are responsivity coefficients for each channel, calculated at 24 degrees C and normalized by the linearity corrected count rate.

S2. Statistics of instrument-pair comparisons

Tables S1, S2 and S3 below provide the per-wavelength and global statistics for the comparisons displayed in Figs. 8, 9 and 10 of the paper.

Table S1. HyperPro vs. C-OPS comparison statistics

λ	N	MAD	MD	MAUPD	MUPD
412	13	0.000210	-0.000074	2.42	-0.84
443	13	0.000238	0.000221	3.45	3.21
465	13	0.000180	0.000148	2.86	2.35
490	13	0.000117	0.000053	2.27	1.00
532	13	0.000064	-0.000042	2.92	-1.94
555	13	0.000050	-0.000033	3.35	-2.29
589	13	0.000026	0.000013	4.30	2.20
625	13	0.000018	0.000013	9.53	7.12
665	13	0.000012	0.000006	11.03	5.14
683	13	0.000015	0.000014	14.98	13.78
694	13	0.000015	0.000014	20.85	19.85
710	13	0.000008	0.000001	22.95	5.11
ALL	156	0.000079	0.000028	8.41	4.56

Table S2. DALEC vs. C-OPS comparison statistics

λ	N	MAD	MD	MAUPD	MUPD
No skylight reflection correction					
412	41	0.000728	-0.000448	8.55	-2.95
443	41	0.000580	-0.000273	8.29	-1.40
465	41	0.000397	0.000048	6.43	3.41
490	41	0.000529	-0.000345	10.11	-3.68
532	41	0.000301	-0.000249	13.22	-8.11
555	41	0.000268	-0.000242	16.86	-12.46
589	41	0.000216	-0.000211	30.52	-27.30
625	41	0.000167	-0.000163	58.00	-53.80
665	41	0.000130	-0.000125	73.75	-66.41
683	41	0.000096	-0.000093	62.69	-56.62
694	41	0.000083	-0.000072	74.25	-52.05
710	41	0.000077	-0.000077	102.94	-100.97
ALL	492	0.000298	-0.000187	38.80	-31.86
Method1					
412	41	0.000777	0.000720	9.58	11.13
443	41	0.000639	0.000586	9.46	11.05
465	41	0.000660	0.000647	10.81	13.11
490	41	0.000302	0.000179	6.03	6.16
532	41	0.000165	0.000109	8.06	7.81
555	41	0.000118	0.000035	8.41	5.08
589	41	0.000077	-0.000018	13.15	0.27

625	41	0.000060	-0.000030	28.68	-7.96
665	41	0.000055	-0.000036	44.25	-19.65
683	41	0.000048	-0.000032	40.18	-19.54
694	41	0.000056	-0.000050	51.82	-41.57
710	39	0.000029	-0.000018	62.15	-24.44
ALL	490	0.000250	0.000175	24.23	-4.80
Method2					
412	41	0.000393	0.000139	4.55	3.80
443	41	0.000319	0.000102	4.47	3.74
465	41	0.000336	0.000224	5.23	6.00
490	41	0.000245	-0.000180	4.69	-0.94
532	41	0.000132	-0.000092	5.97	-1.74
555	41	0.000134	-0.000122	8.73	-5.62
589	41	0.000109	-0.000107	16.74	-14.10
625	41	0.000095	-0.000095	37.75	-35.48
665	41	0.000077	-0.000076	50.92	-48.18
683	41	0.000060	-0.000059	43.84	-40.33
694	41	0.000061	-0.000061	55.40	-52.80
710	40	0.000027	-0.000022	54.76	-38.79
ALL	491	0.000166	-0.000029	24.36	-18.66
Method3					
412	41	0.000547	0.000405	6.44	7.02
443	41	0.000429	0.000298	6.07	6.58
465	41	0.000438	0.000376	6.90	8.46
490	41	0.000185	-0.000062	3.56	1.30
532	41	0.000108	-0.000021	4.97	1.48
555	41	0.000105	-0.000066	6.98	-1.99
589	41	0.000083	-0.000068	13.04	-8.05
625	41	0.000077	-0.000071	30.87	-25.33
665	41	0.000068	-0.000063	44.40	-38.15
683	41	0.000055	-0.000049	38.84	-31.47
694	41	0.000051	-0.000049	46.41	-41.94
710	41	0.000025	-0.000016	54.83	-20.37
ALL	492	0.000181	0.000051	21.94	-11.87
Method4					
412	41	0.000579	0.000431	6.84	7.38
443	41	0.000453	0.000317	6.42	6.90
465	41	0.000458	0.000391	7.24	8.72
490	41	0.000206	-0.000051	3.92	1.53
532	41	0.000120	-0.000016	5.49	1.73
555	41	0.000111	-0.000063	7.38	-1.74
589	41	0.000089	-0.000066	13.80	-7.64
625	41	0.000081	-0.000071	31.71	-24.60
665	41	0.000071	-0.000065	45.48	-37.52
683	41	0.000058	-0.000051	40.13	-31.14
694	41	0.000052	-0.000049	46.50	-41.29
710	39	0.000029	-0.000022	53.15	-31.99
ALL	490	0.000193	0.000057	22.21	-12.39
Method5					
412	41	0.000725	0.000705	9.24	11.20
443	41	0.000554	0.000520	8.40	10.26
465	41	0.000558	0.000552	9.21	11.63
490	41	0.000205	0.000078	4.10	4.19
532	41	0.000116	0.000071	5.52	5.81
555	41	0.000081	0.000009	5.54	3.03
589	41	0.000056	-0.000013	9.33	0.42
625	41	0.000048	-0.000032	21.10	-10.48
665	41	0.000043	-0.000036	31.03	-22.75
683	41	0.000035	-0.000026	27.38	-17.67
694	41	0.000033	-0.000029	33.66	-27.57
710	41	0.000018	-0.000001	52.86	8.74
ALL	492	0.000206	0.000150	18.11	-1.93

Table S3. DALEC vs. HyperPro comparison statistics

λ	N	MAD	MD	MAUPD	MUPD
No skylight reflection correction					
413	12	0.000578	-0.000505	6.86	-7.91
443	12	0.000598	-0.000587	8.67	-11.16
467	12	0.000357	-0.000258	5.79	-6.35
487	12	0.000317	-0.000231	5.95	-6.59
508	12	0.000419	-0.000419	12.04	-12.79
531	12	0.000276	-0.000276	12.07	-12.41
555	12	0.000285	-0.000285	18.09	-15.94
589	12	0.000250	-0.000250	36.87	-33.29
623	12	0.000178	-0.000178	64.81	-63.20
663	12	0.000136	-0.000136	81.47	-77.21
684	12	0.000111	-0.000111	78.22	-61.21
694	12	0.000095	-0.000088	91.37	-68.22
711	12	0.000084	-0.000084	117.04	-116.38
ALL	156	0.000283	-0.000262	41.48	-36.20
Method1					
413	12	0.000656	0.000647	8.16	5.80
443	12	0.000369	0.000251	5.59	1.28
467	12	0.000358	0.000322	6.04	2.91
487	12	0.000295	0.000274	5.78	2.73
508	12	0.000139	0.000030	4.29	0.89
531	12	0.000129	0.000070	6.21	3.17
555	12	0.000076	-0.000020	5.33	0.56
589	12	0.000073	-0.000067	12.31	-8.71
623	12	0.000058	-0.000054	27.56	-23.28
663	12	0.000055	-0.000055	43.79	-36.53
684	12	0.000057	-0.000057	49.10	-41.11
694	12	0.000076	-0.000076	75.79	-71.28
711	12	0.000026	-0.000024	60.94	-46.58
ALL	156	0.000182	0.000096	23.91	-15.41
Method2					
413	12	0.000339	0.000082	4.07	-1.28
443	12	0.000323	-0.000214	4.78	-5.73
467	12	0.000239	-0.000081	3.88	-3.84
487	12	0.000193	-0.000067	3.67	-3.92
508	12	0.000229	-0.000229	6.78	-6.89
531	12	0.000128	-0.000124	5.82	-5.97
555	12	0.000172	-0.000172	11.47	-9.69
589	12	0.000155	-0.000155	24.91	-22.32
623	12	0.000119	-0.000119	49.97	-48.14
663	12	0.000095	-0.000095	67.40	-61.10
684	12	0.000083	-0.000083	65.94	-59.00
694	12	0.000084	-0.000084	83.77	-79.14
711	12	0.000028	-0.000028	64.90	-53.15
ALL	156	0.000168	-0.000105	30.57	-24.11
Method3					
413	12	0.000414	0.000336	4.90	1.75
443	12	0.000232	-0.000028	3.42	-3.04
467	12	0.000193	0.000062	3.11	-1.53
487	12	0.000156	0.000044	2.95	-1.83
508	12	0.000151	-0.000142	4.54	-4.39
531	12	0.000091	-0.000060	4.23	-3.11
555	12	0.000124	-0.000123	8.36	-6.53
589	12	0.000120	-0.000120	19.70	-16.99
623	12	0.000099	-0.000099	41.62	-39.81
663	12	0.000087	-0.000087	59.64	-53.52
684	12	0.000077	-0.000077	59.35	-52.98
694	12	0.000074	-0.000074	75.19	-70.32
711	12	0.000026	-0.000024	60.39	-47.93
ALL	156	0.000142	-0.000030	26.72	-24.03
Method4					
413	12	0.000468	0.000366	5.56	2.15

443	12	0.000226	-0.000006	3.28	-2.69
467	12	0.000201	0.000078	3.25	-1.25
487	12	0.000157	0.000055	2.96	-1.59
508	12	0.000152	-0.000134	4.55	-4.16
531	12	0.000099	-0.000056	4.58	-2.88
555	12	0.000124	-0.000121	8.32	-6.34
589	12	0.000120	-0.000120	19.40	-16.65
623	12	0.000101	-0.000101	40.98	-39.13
663	12	0.000090	-0.000090	59.13	-52.91
684	12	0.000080	-0.000080	59.16	-52.86
694	12	0.000075	-0.000075	74.65	-69.63
711	12	0.000033	-0.000031	64.07	-49.31
ALL	156	0.000148	-0.000024	26.91	-23.78
Method5					
413	12	0.000630	0.000630	8.24	5.95
443	12	0.000286	0.000190	4.63	0.69
467	12	0.000274	0.000235	4.83	1.68
487	12	0.000211	0.000182	4.27	1.08
508	12	0.000105	-0.000027	3.29	-0.79
531	12	0.000084	0.000032	4.05	1.28
555	12	0.000086	-0.000048	6.00	-1.43
589	12	0.000084	-0.000066	14.38	-8.27
623	12	0.000067	-0.000060	30.47	-24.61
663	12	0.000058	-0.000058	44.02	-37.41
684	12	0.000053	-0.000053	45.56	-38.58
694	12	0.000055	-0.000055	61.75	-56.58
711	12	0.000014	-0.000008	43.61	-5.91
ALL	156	0.000154	0.000069	21.16	-13.53

References

1 J. L. Mueller and R. Austin, “Characterization of Oceanographic and Atmospheric Radiometers,” Chapter 3 in Ocean Optics Protocols For Satellite Ocean Color Sensor Validation, Revision 4, Volume II: Instrument Specifications, Characterization and Calibration, J. L. Mueller, G. S. Fargion and C. R. McClain, Editors, NASA/TM-2003-21621/Rev-Vol II, Goddard Space Flight Space Center, Greenbelt, Maryland 20771 (2003).

2 J. Pacheco-Labrador, A. Ferrero, and M. Martín, "Characterizing integration time and gray-level-related nonlinearities in a NMOS sensor," Appl. Opt. **53**, 7778-7786 (2014).

3 G. Zibordi, M. Talone, and L. Jankowski, “Response to Temperature of a Class of In Situ Hyperspectral Radiometers,” J. Atm. Ocean Tech. **34**, 1795-1805 (2017).